Catalysis Today 158 (2010) 296–304

Contents lists available at ScienceDirect

Catalysis Today

journal homepage: www.elsevier.com/locate/cattod

Using TiO_2 photocatalyst with adsorbent to oxidize carbon monoxide in rich hydrogen

Akira Nishimura[a,*], Tomokazu Hisada[a], Masafumi Hirota[a], Mitsuhiro Kubota[b], Eric Hu[c]

[a] Division of Mechanical Engineering, Graduate School of Engineering, Mie University, 1577 Kurimamachiya-cho, Tsu, Mie 514-8507, Japan
[b] Department of Energy Engineering and Science, Graduate School of Engineering, Nagoya University, Furo-cho, Chikusa-ku, Nagoya 464-8603, Japan
[c] School of Mechanical Engineering, The University of Adelaide, SA 5005, Australia

ARTICLE INFO

Article history:
Available online 2 May 2010

Keywords:
TiO_2 photocatalyst
CO oxidization
Silica
H_2
PEFC

ABSTRACT

Polymer electrolyte fuel cell (PEFC) starts to be used in industries and homes in the world. Hydrogen (H_2) is normally used as the fuel to power PEFC. However, the power generation performance of PEFC is harmed by the carbon monoxide (CO) in the H_2 that is often produced from methane (CH_4). Normally, precious metal catalysts and thermal energy are used to remove CO in rich H_2, which are costly. Therefore, an alternative process, i.e. using the TiO_2 photocatalyst combined with adsorbent to oxidize the CO is studied in this paper. The purpose of this study is to understand oxidization characteristics and experimental conditions for the alternative process, in order to improve its efficiency. The impacts of initial concentration ratio of O_2 to CO, filling volume ratio of the TiO_2 particles combined with silica to reactor, and different preparation methods of TiO_2 with adsorbent on the CO oxidization performance are investigated. The optimum initial concentration of O_2 and best filling volume ratio of the TiO_2 particles combined with silica to reactor was found to be 4 vol% and 50 vol%, respectively, under the experimental conditions. By using TiO_2 particles combined with mesoporous silica, the concentration of CO in the reactor was reduced from 10 800 ppmV down to 27 ppmV after UV light illumination of 48 h.

1. Introduction

Polymer electrolyte fuel cell (PEFC) has been developed vigorously in the world since it is an attractive and clean power generation technology. H_2 is used as the fuel to power PEFC. However, there are some barriers blocking the wider application of PEFC among industries and homes in the world. One of the barriers is the reduction of power generation performance when CO exists in the H_2 produced from CH_4, CH_3OH and gasoline.

CH_4 is normally the feedstock to produce H_2 with Ni or Ru catalyst at the high temperature range of 873–973 K through the following reaction:

$$CH_4 + H_2O \rightarrow CO + 3H_2 \quad (1)$$

After this reaction, there is about 10 vol% of CO in the products. The CO concentration can be reduced down to about 1 vol% by the following so called shift reaction:

$$CO + H_2O \rightarrow CO_2 + H_2 \quad (2)$$

After the shift reaction, the concentration of CO needs to be further reduced down to 10 ppmV by the following selective oxidization reaction:

$$CO + (1/2)O_2 \rightarrow CO_2 \quad (3)$$

In the H_2 purification processes mentioned above, precious metal catalysts and thermal energy are used, the processes are costly. An alternative process, i.e. using the TiO_2 photocatalyst combined with adsorbent to oxidize is being developed recently due to its potential cost and energy saving.

TiO_2 can oxidize CO with illuminating ultraviolet (UV) ray (available in sunlight) through the following reaction scheme [1,2]:

Photocatalytic reaction:

$$TiO_2 + h\nu (< 380\,\text{nm}) \rightarrow h^+ + e^- \quad (4)$$

Oxidization of CO:

$$CO + h^+ \rightarrow CO^+ \quad (5)$$

Reduction of O_2:

$$O_2 + e^- \rightarrow O_2^- \quad (6)$$

$$O_2^- + h^+ \rightarrow 2O \quad (7)$$

$$O + e^- \rightarrow O^- \quad (8)$$

* Corresponding author. Tel.: +81 59 231 9747; fax: +81 59 231 9747.
E-mail address: nisimura@mach.mie-u.ac.jp (A. Nishimura).

0920-5861/$ – see front matter © 2010 Elsevier B.V. All rights reserved.
doi:10.1016/j.cattod.2010.03.076

From the products of the reactions, Eqs. (5) and (8), the following combined reaction occurs:

$$CO^{+} + O^{-} \rightarrow CO_2 \quad (9)$$

Therefore, the total reaction scheme can be written as following:

$$CO + (1/2)O_2 \rightarrow CO_2 \quad (10)$$

where $h\nu$ is the energy of UV ray. h^+ and e^- represent the hole and electron produced by photocatalytic reaction, respectively.

The alternative process with TiO_2 has the following merits. (1) There is a lot of TiO_2 reserve in the earth compared with precious metal catalyst. The amount of Ti is the ninth largest among the elements consisting the earth crust [3]. (2) Cost is lower than using precious metal catalyst. (3) Energy consumption is less and the control of the reaction process is easier since high thermal energy is not necessary. (4) Solar energy can be used for the reaction. (5) TiO_2 is stable in both acid and alkali environment.

However, from the calculations by the authors, the mass transfer time of the gases crossing the TiO_2 particles is about 10^5–10^{-1} s which is slower than that of the photo reaction which is about 10^{-9}–10^{-15} s. Therefore, to improve the mass transfer rate, the adsorbent which is able to promote the photocatalytic reaction is introduced in our study.

Literatures survey shows that TiO_2 photocatalyst combined with adsorbent such as activated carbon, zeolite and silica (SiO_2) were mainly used for the development of environmental purification technology such as NO_x removal [4–6], decomposition of acetaldehyde [7], dimethylsulfide [8], 2-propanol [9], degradation of organophosphate and phosphonoglycine [10], and CO_2 reforming into fuel like CH_4 and CH_3OH [11,12]. Some previous studies also reported the oxidization of CO in H_2 using photocatalyst. The CO oxidization characteristics of photocatalyst combined with FeO_x or Al_2O_3 or CeO_x and precious metal catalyst like Pt or Au were reported [13–15]. In addition, the CO oxidization characteristics of Pt loaded on zeolite without photocatalyst were also reported [16,17]. Although there are reports on the CO oxidization characteristics of Mo/SiO_2 or Cr/SiO_2 [18,19], there is no report on the CO oxidization characteristics of TiO_2 combined with adsorbent.

The purpose of this study is to understand the oxidization characteristics and experimental conditions in order to improve the CO oxidization performance of TiO_2 combined with adsorbent. In this study, a silica is selected as adsorbent because UV ray can penetrate through silica, resulting that the particles of TiO_2 combined with silica can be used in a bed type reactor. The comparison of CO oxidization performance under various conditions was carried out in terms of residual ratio of CO, utilization ratio of O_2, selection ratio of CO oxidization, and amount of oxidized CO per unit mass of TiO_2 combined with silica.

2. Experiment

2.1. Characteristics of the TiO_2 combined with silica and preparation method of the mesoporous silica loaded with TiO_2 particles

Two types of TiO_2 particle combined with silica were prepared for CO oxidization in this study. Table 1 lists the physical properties of TiO_2 particle combined with silica used in this study.

The first type is the silica gel particles coated with TiO_2 film (PSB-01, Photocatalyst Laboratory Corp.) which has the following characteristics:

(i) TiO_2 film is coated on the surface of silica gel particle. Therefore, the amount of TiO_2 is large and adsorption performance is low due to the blockage of the pores of silica gel by the TiO_2 film coated. The crystallization of TiO_2 coated on the particles is in anatase form, which is proved by the XRD (X-ray diffraction, MiniFlex II, Rigaku Corp.) pattern as shown in Fig. 1. From this figure, the peak of $2\theta = 25^\circ$ which means the crystallization of anatase form of TiO_2 can be seen clearly.

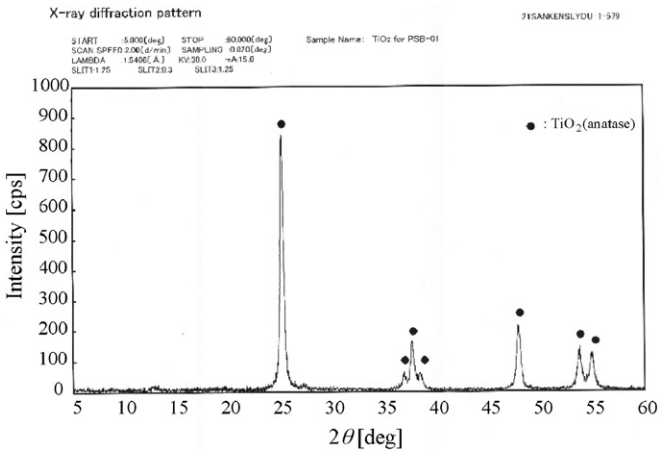

Fig. 1. XRD pattern of TiO_2 film coated on silica gel particle.

(ii) The photocatalytic reaction is expected to occur on the surface only.

(iii) Average pore size is much larger than the molecular diameter of CO and O_2 which is 0.38 nm and 0.35 nm, respectively. Therefore, the adsorption performance is expected low.

The other type is the mesoporous silica particles loaded with TiO_2, which have the following characteristics:

(i) The ratio of loaded TiO_2 can be controlled from the viewpoint of qualitative evaluation.

(ii) Average pore diameter is in nano-scale. Since the molecular diameter of CO and O_2 is relatively closed to the average pore diameter, the high adsorption performance is expected.

(iii) TiO_2 particle is located inside of pores of the mesoporous silica. Light can pass through mesoporous silica and gases can also get into the pores of mesoporous silica through the diffusion, therefore, good photocatalytic reaction as well as good adsorption performance can be expected.

Fig. 2 shows the preparation method of mesoporous silica particles loaded with TiO_2 in our laboratory, which is developed by referring the literature [20–22]. P25 (Degussa, P25, Japan Aerosil Corp., Ltd.) powder was selected as TiO_2 source to load, P25 that has high reactivity, consists of anatase and rutile crystallization form of TiO_2. Because of the primary particle size of P25 which is ranged between 20 nm and 30 nm, P25 is suitable for being inserted into the mesoporous silica whose size is ranged between 30 nm and 100 nm generally. P25 plays the role of the core for forming mesoporous silica. The pores of mesoporous silica are formed to or around the particles of P25. The ratio of loaded TiO_2 to mesoporous silica was controlled by the amount of P25 added to the mixture solution of ion-exchange water, $CH_3(CH_2)_{15}N(CH_3)_3Br$ (purity of 99 wt%, Nacalai Tesque Corp.), $(C_2H_5O)_4Si$ (purity of 95 wt%, Nacalai Tesque Corp.) and NH_3 (purity of 28 wt%, Nacalai Tesque Corp.). The amount of P25 particle added to the mixture solution was 0.54 g, 0.86 g, 2.10 g, 7.30 g and 19.5 g for the ratio of 10 wt%, 15 wt%, 30 wt%, 60 wt% and 80 wt%, respectively. Here, the ratio of loaded TiO_2 is named after preparation condition since it is very difficult to measure the weight of TiO_2 in mesoporous silica directly after

Table 1
Physical properties of TiO_2 particle combined with silica used in this study.

	Silica gel particle coated with TiO_2 film	Mesoporous silica loaded with TiO_2 particles
Particle size (mm)	1.7–4.0	0.03–0.25 (primary particle) 2.0–5.6 (agglomerated particle)
Specific surface area (m^2/g)	200	219–1038
Average pore diameter (nm)	15	2.7–3.1
Pore volume (mL/g)	0.8	0.63–0.94
Ratio of loaded TiO_2 (wt%)	10–11	0–80

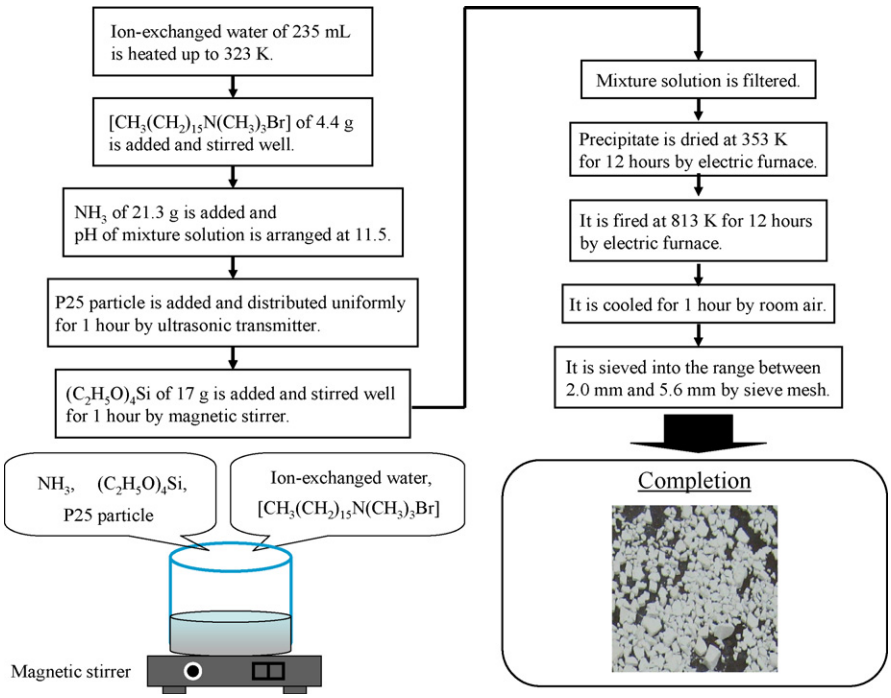

Fig. 2. Preparation method of mesoporous silica loaded with TiO_2 particles.

preparation process. Particle size of agglomerated mesoporous silica particles loaded with TiO_2 was sieved into the range between 2.0 mm and 5.6 mm after burning.

The sample of mesoporous silica particles loaded with TiO_2 prepared was analyzed by XRD (X-ray diffraction, Ultima IV, Rigaku Corp.), TEM (transmission electron microscope, H-800, Hitachi Corp.) and N_2 adsorption isotherms measurement system (Autosorb-1-MP, Sysmex Corp.) to determine its chemical and physical properties including crystallization characteristics of silica and TiO_2, primary particle size, shape of mesoporous silica, the amount of TiO_2 particle in the mesoporous silica, pore diameter distribution, pore volume and specific surface area.

2.2. Experimental apparatus and procedure

Fig. 3 illustrates the experimental apparatus which consists of a reactor, a gas mixing chamber, a mass flow controller (MODEL 3660, KOFLOC), a regulator and a gas cylinder. The reactor, which is a batch type, consists of stainless steel pipe (450 mm (L) × 60.5 mm (OD) × 2.5 mm (t)), gas supply and exhaust pipe, valves, gas sampling tap and UV lamp (FL15BLB, Toshiba Co., 436 mm (L) × 25.5 mm (D)) located at the center of stainless steel pipe. The space for charging gas and filling TiO_2 particles is 6.35×10^5 mm^3. The central wavelength and mean light intensity of UV light is 352 nm and 4.34 mW/cm^2, respectively. This light intensity is almost the same as the UV intensity in solar radiation at daytime in the summer of Japan.

In the experiment, O_2 (purity of 99.9999 vol%) and the premixed gas of H_2 and CO (H_2: 99 vol%, CO: 1 vol%) were mixed in the gas mixing chamber before supplied to the reactor. By adjusting the flow rate and the pressure of the gas, the initial concentration ratio

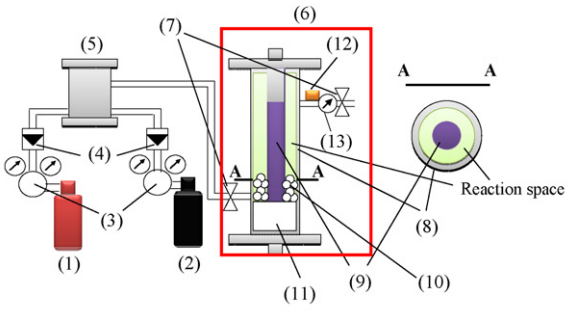

Fig. 3. Experimental apparatus.

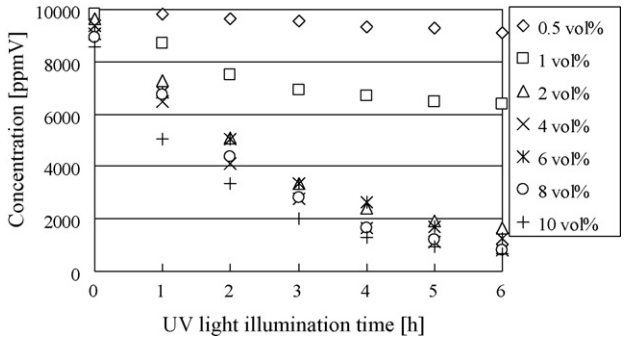

Fig. 4. Change of concentration of CO with UV light illumination time for different initial concentrations of O_2.

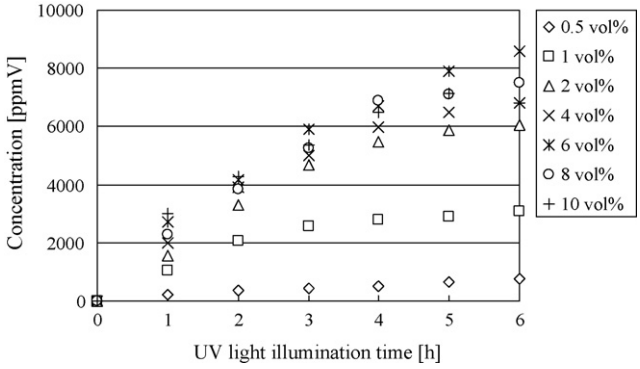

Fig. 5. Change of concentration of CO_2 with UV light illumination time for different initial concentrations of O_2.

of O_2 to CO could be controlled. This remixed gas was charged into the reactor, and the concentration and pressure of gases were confirmed before starting the experiment. The ratios of gasses were charged as follows:

$$CO : O_2 = 1 : 0.5,\ 1 : 1,\ 1 : 2,\ 1 : 4,\ 1 : 8,\ \text{and}\ 1 : 10\ (\text{balanced by}\ H_2)$$

Although 1 mol CO reacts with 0.5 mol O_2 theoretically as shown in the reaction of Eq. (10), it is necessary to confirm the practical optimum initial concentration ratio of O_2 to CO in rich H_2 environment.

The total pressure in the reactor was set at 0.1 MPa. The gas temperature in the reactor was kept at about 300 K during the experiment. Particles of TiO_2 combined with silica were filled into the rector before gas was supplied. The particles of TiO_2 combined with silica were filled into the reactor from 10 vol% to 50 vol% of full reactor volume size.

The experiment was started when illumination of UV light was applied. The gas in reactor was sampled hourly during the experiment. The gas samples were analyzed by TCD gas chromatograph (VARIAN micro-GC CP-4900, GL Science Corp.) equipped with double columns of Molsieve 5A and PoraPLOT Q. The minimum resolution of this gas chromatograph is 1 ppmV.

3. Results and discussion

3.1. Effect of initial ratio of O_2 to CO on CO oxidization performance with silica gel coated with TiO_2 film

Figs. 4 and 5 show the concentration change of CO and CO_2 with UV light illumination time for the different initial concentrations of O_2. Silica gel particles coated with TiO_2 film was used in the experiment. The filling volume ratio of the particles of TiO_2 combined with silica to the reactor was set at 50 vol%. From these figures, it can be

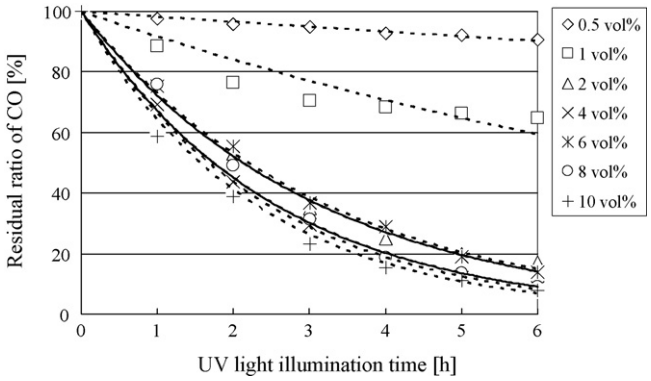

Fig. 6. Change of residual ratio of CO with UV light illumination time for different initial concentrations of O_2.

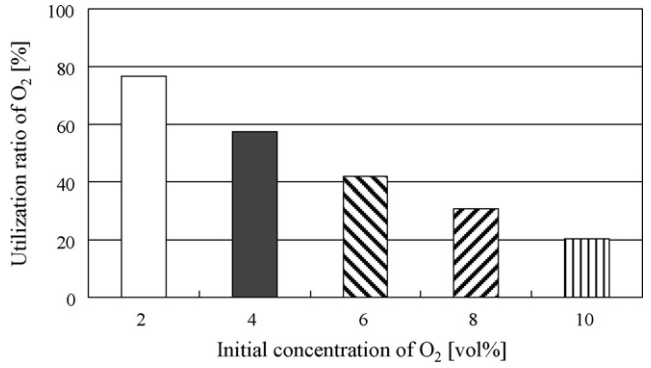

Fig. 7. Comparison of utilization ratio of O_2 among different initial concentrations of O_2.

seen that the concentration of CO has been oxidized in all cases. To compare the oxidization rate of CO, Fig. 6 shows the change of residual ratio of CO with UV light illumination time for different initial concentrations of O_2. The residual ratio of CO is defined as:

$$R_{\text{res-CO}} = \frac{[\text{CO}]}{[\text{CO}]_0} \times 100 \tag{11}$$

where $R_{\text{res-CO}}$ stands for the residual ratio of CO (%), [CO] is the concentration of CO at each time (ppmV), $[CO]_0$ is the initial concentration of CO at the beginning of the experiment (ppmV). Regression line is derived according to the tendency of data plot:

$$R_{\text{res-CO}} = 100e^{-\alpha t} \tag{12}$$

where α is the coefficient of CO removal (1/h) and t is the time for UV light illumination (h).

Fig. 6 shows the rate of the CO residual ratio change becomes more rapidly with the increase of initial concentration of O_2 up to 4 vol%. Therefore, it is confirmed that the initial concentration of O_2 larger than the stoichiometric ratio (that is 0.5 vol%) is necessary. However, the rate increase becomes flat beyond 4 vol%. The α value, i.e. Eq. (12), which indicates the oxidization rate of CO is 0.017, 0.087, 0.317, 0.416, 0.326, 0.400 and 0.445 for initial concentration of O_2 of 0.5 vol%, 1 vol%, 2 vol%, 4 vol%, 6 vol%, 8 vol% and 10 vol%, respectively. From these results, the initial concentration of O_2 at about 4 vol% is thought to be optimum under the study conditions.

Fig. 7 shows the comparison of utilization ratio of O_2 with different initial concentrations of O_2. In Fig. 7, the data on initial concentration of O_2 of 0.5 vol% and 1 vol% are omitted since the performance of CO oxidization is very poor as shown in Fig. 6. The

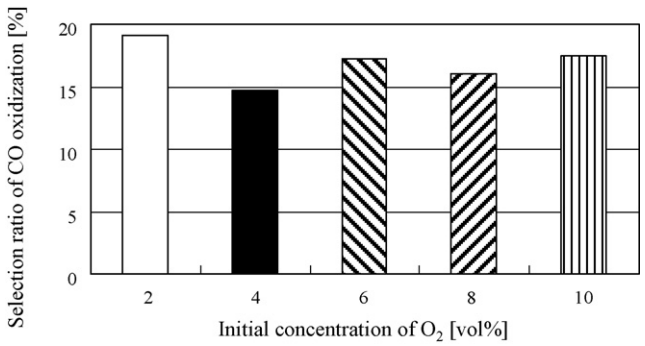

Fig. 8. Comparison of selection ratio of CO oxidization among different initial concentrations of O_2.

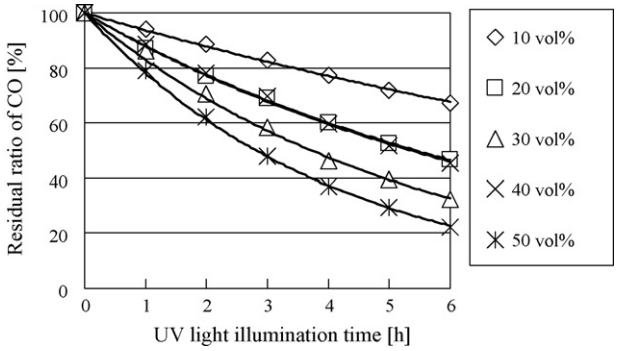

Fig. 9. Change of residual ratio of CO with UV light illumination time for different filling volume ratios of the particles of silica gel coated with TiO_2 film to reactor.

utilization ratio of O_2 is defined as:

$$R_{\text{uti-O}_2} = \frac{[O_2]_0 - [O_2]}{[O_2]_0} \times 100 \quad (13)$$

where $R_{\text{uti-O}_2}$ stands for the utilization ratio of O_2 (%), $[O_2]_0$ is the initial concentration of CO at the beginning of the experiment (ppmV), $[O_2]$ is the concentration of O_2 at each time (ppmV). In Fig. 7, $[O_2]$ after UV light illumination of 6 h is used for calculating $R_{\text{uti-O}_2}$.

It can be seen that the utilization ratio of O_2 is decreased with the increase in initial concentration of O_2. Although the utilization ratio of O_2 of 100% is ideal from the viewpoint of effective utilization of O_2, the optimum initial concentration of O_2 should be decided by also considering the other evaluation factors.

Fig. 8 shows the comparison of selection ratio of CO oxidization among different initial concentrations of O_2. The selection ratio of CO oxidization is:

$$R_{\text{sel-CO}} = \frac{[CO_2] - [CO_2]_0}{2([O_2]_0 - [O_2])} \times 100 \quad (14)$$

where $R_{\text{sel-CO}}$ stands for the selection ratio of CO oxidization (%), $[CO_2]$ is the concentration of CO_2 at each time (ppmV), $[CO_2]_0$ is the initial concentration of CO_2 at the beginning of the experiment (ppmV). In other words, the selection ratio of CO oxidization means the ratio of amount of O_2 used for CO oxidization to total amount of reduced O_2. As shown in Eq. (10), 1 mol CO reacts with 0.5 mol O_2 to produce 1 mol CO_2. To adjust the volume of reactant and product with consideration of difference in mol numbers, multiplication factor 2 is introduced to the amount of consumed O_2 which is $[O_2]_0$–$[O_2]$ in Eq. (14). In Fig. 8, [CO] and $[O_2]$ after UV light illumination of 6 h are used for calculating $R_{\text{sel-CO}}$.

Fig. 8 shows the selection ratio of CO oxidization is not sensitive to the initial concentrations of O_2 and is at about 15% for all conditions.

Based on results shown in Figs. 6–8, the optimum initial concentration of O_2 is decided to be at 4 vol% in this study for the best reaction rate and utilization ratio of O_2.

3.2. Effect of filling volume ratio on CO oxidization performance

Fig. 9 shows curves of the oxidization rates of CO versus the different filling volume ratios of the silica gel coated with TiO_2 film to reactor. In this experiment, the initial concentration of O_2 was set at 4 vol%. According to Fig. 9, the slope of regression line for the change of residual ratio of CO with UV light illumination time becomes more rapidly with the increase in filling volume ratio. This result indicates that the filling volume ratio of 50% may be the best one for quick CO oxidization. However, the optimum filling volume ratio will be decided after the evaluation of other factors.

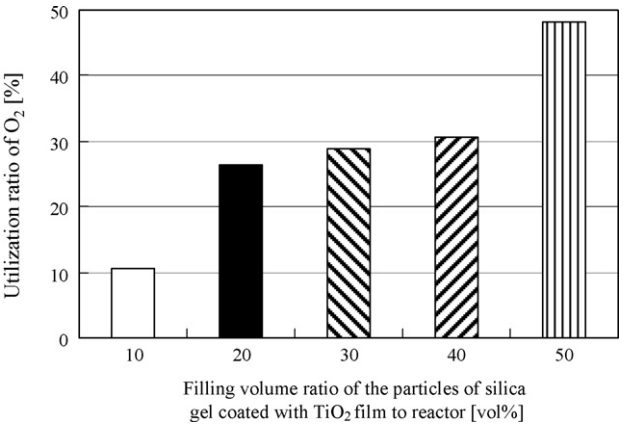

Fig. 10. Comparison of utilization ratio of O_2 among different filling volume ratios of the particles of silica gel coated with TiO_2 film to reactor.

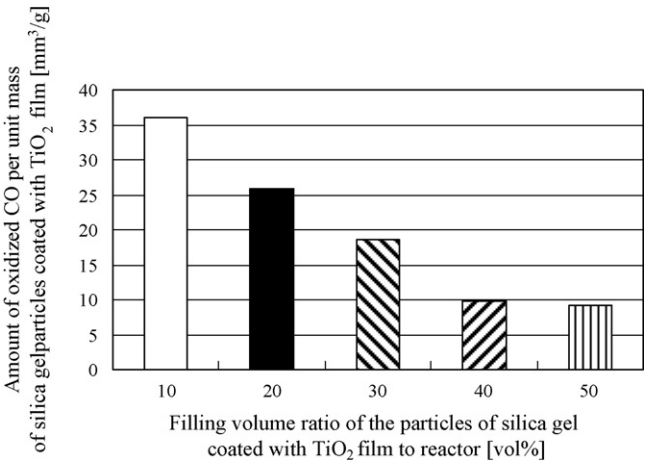

Fig. 11. Comparison of amount of oxidized CO per unit mass of silica gel particles coated with TiO_2 film among different filling volume ratios of the particles of silica gel coated with TiO_2 film to reactor.

Fig. 10 shows the utilization ratio of O_2 in comparison with different filling volume ratios. In Fig. 10, $[O_2]$ value used for calculating $R_{\text{uti-O}_2}$ is the one at UV light illumination of 6 h. The results show that the utilization ratio of O_2 increases with the increase of filling volume ratio.

Fig. 11 shows the relationship between the amount of oxidized CO per unit mass of silica gel particles coated with TiO_2 film and the filling volume ratio. In Fig. 11, [CO] after UV light illumination of 6 h is used for calculating the amount of oxidized CO. It can be seen that the amount of oxidized CO per unit mass decreases with

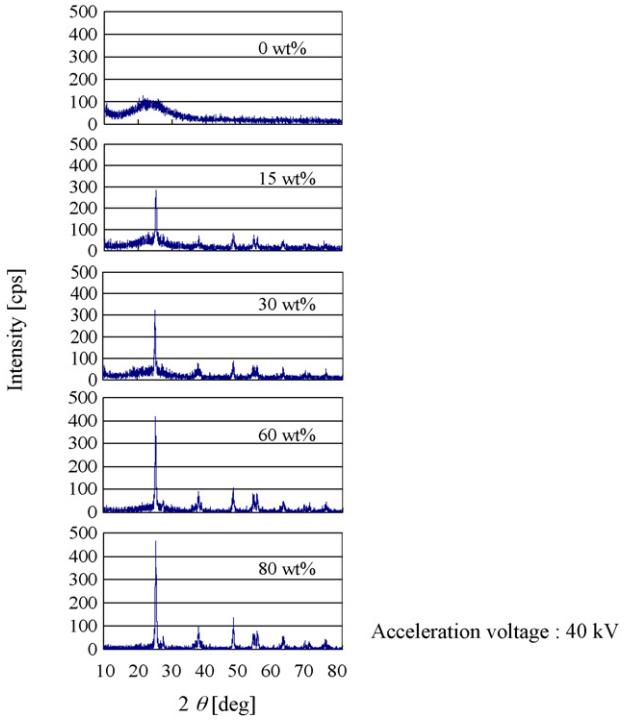

Fig. 12. XRD patterns of mesoporous silica loaded with TiO_2 particles for the ratio of loaded TiO_2 of 0 wt%, 15 wt%, 30 wt%, 60 wt% and 80 wt%.

the increase of filling volume ratio, which reaches the lowest value when the filling volume ratio is at about 40 vol%. The reason of this is thought to be that the gas diffusion rate through the bed of particles of TiO_2 combined with silica is slow and the most of the gases in the reactor might not get chances to even in contact with the particles.

According to the results shown in Figs. 9–11, the filling volume ratio of 50 vol% is selected for further experiment in this study, as a compromise between oxidization rate of CO and utilization ratio of O_2.

3.3. Effect of the loading method on CO oxidization performance

To confirm the existence of TiO_2 in mesoporous silica and its crystallization characteristics, XRD analysis was performed first. Fig. 12 shows XRD patterns for the ratio of loaded TiO_2 of 0 wt%, 15 wt%, 30 wt%, 60 wt% and 80 wt%. It can be seen that there is the difference in peak distribution between 0 wt% and the other wt%. If the peaks of $2\theta = 25^\circ, 38^\circ, 54^\circ, 63^\circ, 70^\circ, 75^\circ$ were found, they mean that there are both anatase form and rutile form crystallization of TiO_2 in the samples [5,9,23]. These peaks are not found in the pure silica, i.e. with loaded TiO_2 of 0 wt%, as expected. In addition, the height of the highest peak on TiO_2 in XRD pattern becomes higher with the increase of the ratio of loaded TiO_2. Fig. 13 shows the correlation between the ratio of loaded TiO_2 and the value of highest peak on TiO_2 in each XRD pattern. The height of the highest peak in XRD patterns increases proportionally with the increase in the ratio of loaded TiO_2. Therefore, the ratio of loaded TiO_2 can be controlled by this preparation method from the viewpoint of qualitative evaluation. In this figure, the broad peak around $2\theta = 25^\circ$ indicates the amorphous form of mesoporous silica.

To check the size and physical structure of the mesoporous silica loaded with TiO_2 particles, TEM analysis was performed. Figs. 14–18 show the TEM images for the ratios of loaded TiO_2 of 0 wt%, 15 wt%, 30 wt%, 60 wt% and 80 wt%. According to these figures, the black small spheres are observed in mesoporous silica

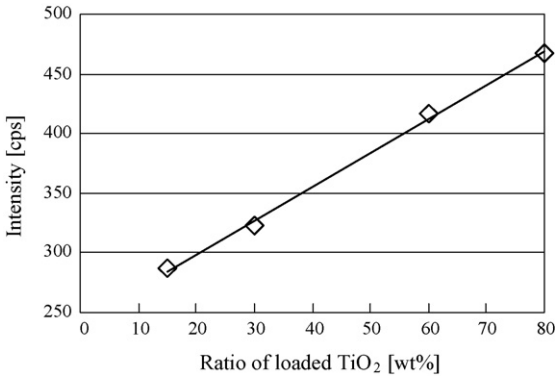

Fig. 13. Relationship between the ratio of loaded TiO_2 and the value of highest peak for each XRD pattern.

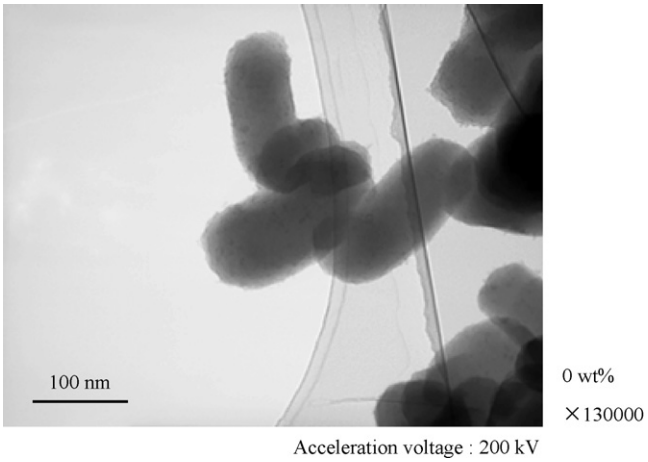

Fig. 14. TEM images of mesoporous silica loaded with TiO_2 particles for the ratio of loaded TiO_2 of 0 wt%.

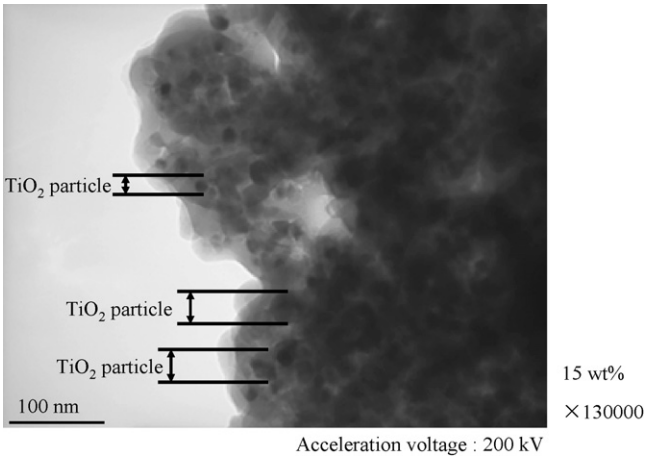

Fig. 15. TEM images of mesoporous silica loaded with TiO_2 particles for the ratio of loaded TiO_2 of 15 wt%.

except for the ratio of loaded TiO_2 of 0 wt%. The diameters of these black small spheres are about 20–30 nm which is equal to the primary diameter of P25 particles. According to [22], the black small spheres in mesoporous silica gel in the TEM images are TiO_2 particles. Some particles over 20–30 nm are observed in Figs. 15–18 which indicate the agglomeration of TiO_2 particles in the mixture solution during preparation process might occur. The agglomeration of TiO_2 particles makes the quantitative control of the ratio

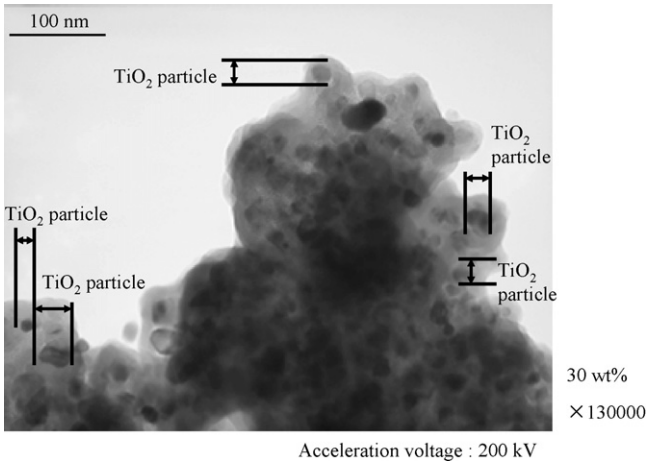

Fig. 16. TEM images of mesoporous silica loaded with TiO_2 particles for the ratio of loaded TiO_2 of 30 wt%.

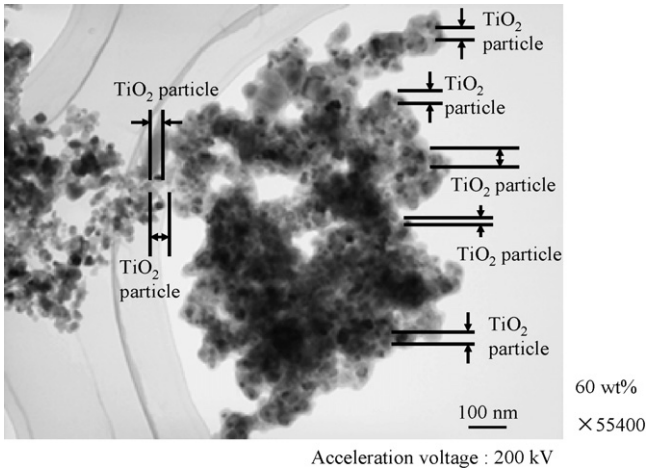

Fig. 17. TEM images of mesoporous silica loaded with TiO_2 particles for the ratio of loaded TiO_2 of 60 wt%.

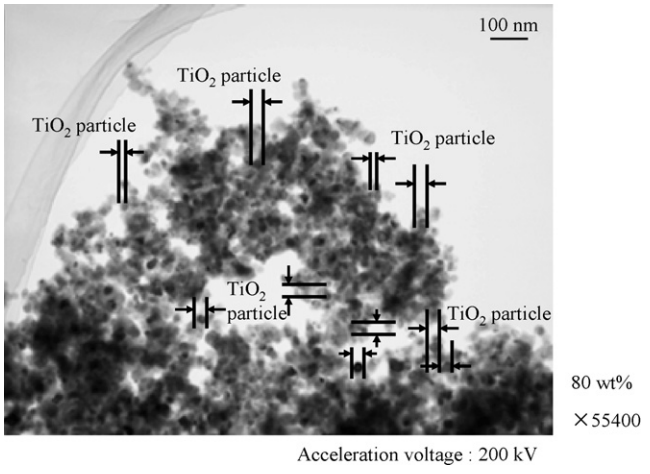

Fig. 18. TEM images of mesoporous silica loaded with TiO_2 particles for the ratio of loaded TiO_2 of 80 wt%.

of loaded TiO_2 difficult. The figures also show the number of TiO_2 particles in TEM images increases with the increase of the loading ratio of TiO_2. Therefore, it proves that mesoporous silica has been successfully loaded with TiO_2 particles through this preparation approach. It can also be seen that the primary diameter of meso-

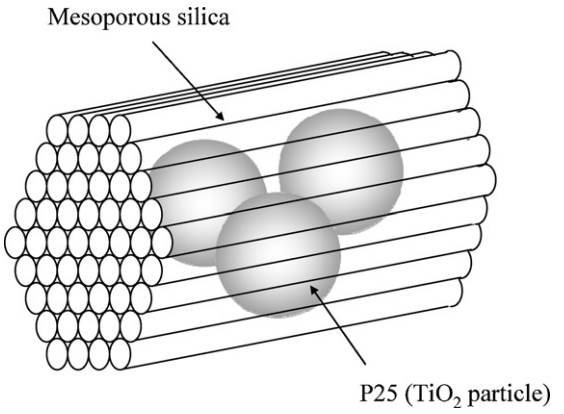

Fig. 19. Schematic drawing of mesoporous silica loaded with TiO_2 particles.

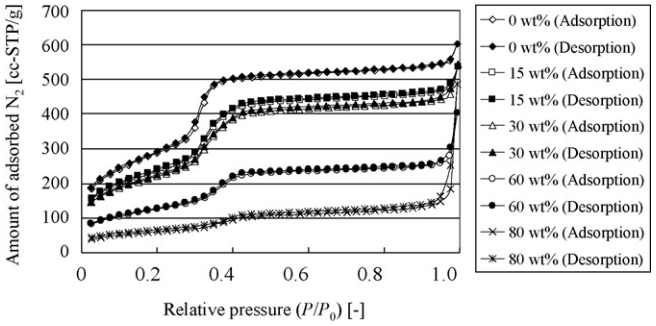

Fig. 20. Comparison of N_2 adsorption and desorption isotherms among the ratio of loaded TiO_2 of 0 wt%, 15 wt%, 30 wt%, 60 wt% and 80 wt%.

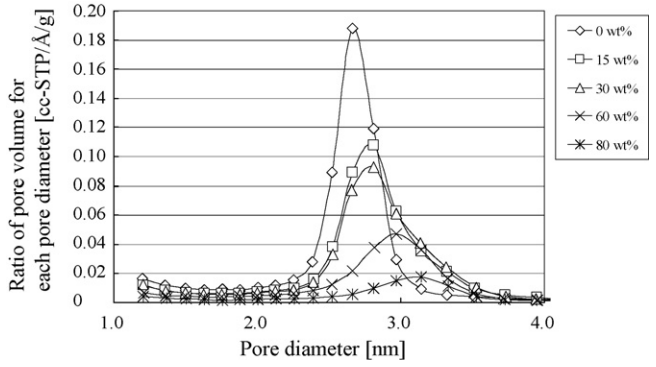

Fig. 21. Pore diameter distribution of mesoporous silica for the ratio of loaded TiO_2 of 0 wt%, 15 wt%, 30 wt%, 60 wt% and 80 wt%.

porous silica decreases gradually with the increase of the loading ratio of TiO_2. When the number of TiO_2 particles loaded in mesoporous silica increases, the honeycomb shape of mesoporous silica which is illustrated in Fig. 19 [22] weakens and breaks due to excess occupation of TiO_2 particles.

Fig. 20 shows the N_2 adsorption and desorption isotherms of the silica for the various ratios of loaded TiO_2. It is confirmed that the adsorption hysteresis is quite small and the obtained N_2 adsorption and desorption isotherms are unique to mesoporous silica. In addition, it reveals that the amount of adsorption is decreased with the increase of loading ratio. The specific surface areas are 1038 m^2/g, 847 m^2/g, 797 m^2/g, 453 m^2/g and 219 m^2/g for the ratio of loaded TiO_2 of 0 wt%, 15 wt%, 30 wt%, 60 wt% and 80 wt%, respectively. Fig. 21 shows the pore diameter distribution of mesoporous silica for the various loading ratios. It can be seen that the pore diameter becomes larger with the increase of the loading ratio. The

Table 2
Comparison of CO oxidization performance of mesoporous silica loaded with TiO_2 particles among different ratios of loaded TiO_2.

	Ratio of loaded TiO_2 (wt%)					
	0	10	15	30	60	80
Concentration of CO at experiment start (ppmV)	11 317	13 220	9257	10 545	9040	10 994
Concentration of CO after UV light illumination of 6 h (ppmV)	11 289	9811	8571	7182	7234	9132
Residual ratio of CO	99.9	74.2	92.6	68.1	80.0	83.1
Utilization ratio of O_2	–	15.7	45.6	16.5	16.8	6.30
Selection ratio of CO oxidization	–	52.0	32.5	40.4	18.6	48.8

Table 3
Comparison of CO oxidization performance between mesoporous silica loaded with TiO_2 particles and silica gel particle coated with TiO_2 film.

Type of TiO_2 combined with silica	Mesoporous silica loaded with TiO_2 particles	Silica gel particle coated with TiO_2 film
Concentration of CO at experiment start (ppmV)	13 220	9384
Concentration of CO after UV light illumination of 6 h (ppmV)	9811	825
Residual ratio of CO	74.2	8.79
Utilization ratio of O_2	15.7	57.5
Selection ratio of CO oxidization	52.0	14.8

The ratio of loaded TiO_2 for mesoporous silica loaded with TiO_2 particles is 10 wt%.

reason may be that pore diameter expands by increased number of TiO_2 particles loaded into the mesoporous silica. Considering these results, it can be concluded that the adsorption performance of mesoporous silica loaded with TiO_2 particles is dropped with the increase in ratio of loaded TiO_2 due to the weakening of the honeycomb shape of mesoporous silica by increased loaded TiO_2.

Table 2 lists the concentrations of CO after UV light illumination of 6 h, for various loading ratios of TiO_2. The 10 wt% ratio was prepared for comparison with the result of silica gel particle coated with TiO_2 film. In this experiment, the initial concentration of O_2 and filling volume ratio were set at 4 vol% and 50 vol%, respectively. Although the mesoporous silica loaded with 0 wt%, i.e. nil TiO_2 particles did not perform CO oxidization as expected, the data of concentration of CO and residual ratio of CO are still listed in this table for reference. The table shows that CO oxidization performance of mesoporous silica loaded with TiO_2 particles is generally not good regardless of the ratio of loaded TiO_2. Among the different loading ratios, 30 wt%, 15 wt% and 10 wt% gives the relatively best residual ratio of CO, utilization ratio of O_2 and selection ratio of CO oxidization, respectively. Therefore, it is clear that the optimum ratio of loaded TiO_2 is in the medium ratio range. The reason is thought to be that the photocatalytic reaction performance is promoted with the increase in loading ratio due to increase in the number of TiO_2 particles, while, according to TEM analysis and N_2 adsorption isotherms, the adsorption performance is dropped with the increase in loading ratio of TiO_2. Consequently, the medium loading ratio of TiO_2 is thought to be the optimum condition.

Table 3 shows the comparison of the CO oxidization performance, after UV light illumination of 6 h, between mesoporous silica loaded with TiO_2 particles and silica gel particles coated with TiO_2 film. In this table, the data is for the mesoporous silica loaded with TiO_2 particles of 10 wt% (to match for the ratio of coated TiO_2 film), initial concentration of O_2 of 4 vol% and filling volume ratio of 50 vol%. The CO oxidization performance of silica gel particle coated with TiO_2 film is generally better than that of mesoporous silica loaded with TiO_2 particles in all aspects except for selection ratio of CO oxidization. This may be caused by that TiO_2 is better positioned on the surface through coating than loading. The amounts of oxidized CO per unit mass of TiO_2 after UV light illumination of 6 h, for silica loaded with TiO_2 particles and coated with TiO_2 film are 672 mm^3/g and 133 mm^3/g, respectively. In other words, loading is the more effective way to make use of TiO_2 for this purpose.

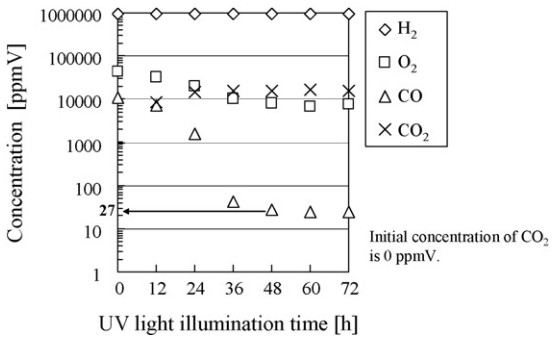

Fig. 22. Change of each gas concentration with UV light illumination time in the long time experiment for mesoporous silica loaded 15 wt% with TiO_2 particles.

Fig. 22 shows that CO concentration with loaded TiO_2 of 15 wt% was decreased down to 27 ppmV after UV light illumination of 48 h, and further down to 24 ppmV after UV light illumination of 72 h. Although taking liger time, the level of oxidized CO finally reached is comparable to the other CO oxidization processes. Consequently, this proposed technology of TiO_2 combined with silica is a promising alternative CO oxidization process.

However, the above results also reveal that the new preparation method to combine TiO_2 with silica may be needed in order to promote the CO oxidization performance. For example, finer TiO_2 particles or fine metal can be loaded at the spots on the surface of mesoporous silica. Finer TiO_2 particles and fine metal loaded on the surface of mesoporous silica support the reaction due to the increase in amount of TiO_2 and prevention of recombination of hole and electron [24–29] without disturbing gas adsorption. The improvement of CO oxidization performance then can be expected.

4. Conclusions

Based on the above experimental results and discussion, the following conclusions can be drawn.

Under the experimental conditions:

(I) The optimum initial concentration of O_2 is 4 vol% from the viewpoint of best matching of reaction rate and utilization ratio of O_2.

(II) The best filling volume ratio of the particles of silica gel coated with TiO_2 film to reactor is 50 vol% from the viewpoint of best matching of oxidization rate of CO, utilization ratio of O_2 and amount of oxidized CO per unit mass of silica gel particles coated with TiO_2 film.

(III) For the mesoporous silica loaded with TiO_2 particles, the photocatalytic reaction performance is promoted with the increase of amount of the loaded TiO_2. However, the adsorption ability decreases with the increase of loaded TiO_2.

(IV) The concentration of CO was reduced from 10 800 ppmV down to 27 ppmV after UV light illumination of 48 h, which is the level comparable with other CO removal methods.

References

[1] M. Formenti, S.J. Teichner, Catalysis 2 (1978) 95.
[2] S. Sato, T. Kadowaki, K. Yamaguchi, Catalyst 27 (1985) 204.
[3] U.S. Department of the Interior, U.S. Geological Survey, Mineral Commodity Summaries 2006, United States Government Printing Office, Washington, D.C., 2006, p. 1.
[4] J. Zhang, M. Minagawa, M. Matsuoka, H. Yamashita, M. Anpo, Catal. Lett. 66 (2000) 241.
[5] H. Kominami, K. Yukishita, T. Kimura, M. Matsubara, K. Hashimoto, Y. Kera, B. Otani, Top. Catal. 47 (2008) 155.
[6] T.H. Lim, S.D. Kim, J. Chin. Inst. Chem. Eng. 36 (2005) 85.
[7] Y.G. Shul, H.J. Kim, S.J. Haam, H.S. Han, Res. Chem. Intermed. 29 (2003) 849.
[8] C. Cantau, T. Pigot, R. Brown, P. Mocho, M.T. Maurette, F. Benoit-Marque, S. Lacombe, Appl. Catal. B: Environ. 65 (2006) 77.
[9] K. Yamaguchi, K. Inumaru, Y. Oumi, T. Sano, S. Yamanaka, Microporous Mesoporous Mater. 117 (2009) 350.
[10] G.R.M. Echavia, F. Matzusawa, N. Negishi, Chemosphere 76 (2009) 595.
[11] K. Ikeue, H. Yamashita, M. Anpo, Electrochemistry 70 (2002) 402.
[12] H. Yamashita, 80th CATSJ Meeting Abstracts 39 (1997) 414.
[13] K. Tanaka, Y. Moro-oka, K. Ishigure, T. Yajima, Y. Okabe, Y. Kato, H. Hamano, S. Sekiya, H. Tanaka, Y. Matsumoto, H. Koinuma, H. He, C. Zhang, Q. Feng, Catal. Lett. 92 (2004) 115.
[14] M. Shou, K. Tanaka, Y. Yoshida, Y. Moro-oka, S. Nagano, Catal. Today 90 (2004) 255.
[15] K. Tanaka, M. Shou, 96th CATST Meeting Abstracts 47 (2005) 418.
[16] M. Watanabe, H. Uchida, H. Igarashi, M. Suzuki, Chem. Lett. (1994) 21.
[17] H. Igarashi, H. Uchida, M. Suzuki, Y. Sasaki, M. Watanabe, Appl. Catal. A: Gen. 159 (1997) 159.
[18] T. Kamegawa, R. Takeuchi, M. Matsuoka, M. Anpo, Catal. Today 111 (2006) 248.
[19] T. Kamegawa, M. Matusoka, M. Anpo, Res. Chem. Intermed. 34 (2008) 427.
[20] K. Inumaru, M. Murashima, T. Kasahara, S. Yamanaka, Appl. Catal. B: Environ. 52 (2004) 275.
[21] T. Kasahara, K. Inumaru, S. Yamanaka, Microporous Mesoporous Mater. 76 (2004) 123.
[22] K. Inumaru, T. Kasahara, M. Yasui, S. Yamanaka, Chem. Commun. (2005) 2131.
[23] K. Takanabe, K. Nagaoka, K. Nariai, K. Aika, J. Catal. 230 (2005) 75.
[24] A. Nishimura, N. Sugiura, M. Fujita, S. Kato, S. Kato, Kagaku Kogaku Ronbunshu 33 (2007) 146.
[25] A. Nishimura, N. Sugiura, M. Fujita, S. Kato, S. Kato, Kagaku Kogaku Ronbunshu 33 (2007) 432.
[26] A. Nishimura, M. Fujita, S. Kato, Proc. 6th Asia Pacific Conference on Sustainable Energy and Environmental Technologies, May 7–11, 2007.
[27] A. Nishimura, N. Sugiura, M. Fujita, S. Kato, AIAA Meeting Papers on Disc of 3rd International Energy Conversion Engineering Conference, August 15–18, 2005, AIAA 2005-5536.
[28] T. Ibusuki, K. Tabata, Catalyst 39 (1997) 24.
[29] Y. Nosaka, A. Nosaka, Introduction of Photocatalyst, 1st ed., Tokyotosho, Tokyo, 2004, p. 151.